PDB
PROTEIN DATA BANK

Structure Explorer - 1PIN

Summary Information

Summary Information

View Structure

Download/Display File

Structural Neighbors

Geometry

Other Sources

Sequence Details

Structure Factors
(compressed)

Explore
SearchLite SearchFields

Title: **Pin1 Peptidyl-Prolyl Cis-Trans Isomerase From Homo Sapiens**

Compound: **Mol_Id: 1; Molecule: Peptidyl-Prolyl Cis-Trans Isomerase; Chain: A; Synonym: Pin1; Ec: 5.2.1.8; Engineered: Yes**
Mol_Id: 2; Molecule: Ala-Pro Dipeptide; Chain: B; Engineered: Yes

Authors: **J. P. Noel, R. Ranganathan, T. Hunter**

Exp. Method: **X-ray Diffraction**

Classification: **Complex (Isomerase/Dipeptide)**

EC Number: **5.2.1.8 (Peptidylprolyl isomerase)**

Source: **Homo sapiens**

Primary Citation: **Ranganathan, R., Lu, K. P., Hunter, T., Noel, J. P.: Structural and functional analysis of the mitotic rotama: Pin1 suggests substrate recognition is phosphorylation dependent. *Cell* 89 *pp.* 875 (1997)**
[Medline]

Deposition Date: **21-Jun-1998** *Release Date:* **14-Oct-1998**

Resolution [Å]: **1.35** *R-Value:* **0.223**

Space Group: **P 4_3 2_1 2**

Unit Cell: *dim [Å]:* *a* **49.00** *b* **49.00** *c* **137.80**
angles [°]: *alpha* **90.00** *beta* **90.00** *gamma* **90.00**

Polymer Chains: **A, B** *Residues:* **165**

Atoms: **1458**

HET groups:

ID (needs Rasmol)	*Name*	*Formula*	*Retriev All PDB IL Containi*
1PG	REPRESENTATIVE POLYETHYLENE GLYCOL FRAGMENT	$2(C_{11}H_{24}O_6)$	1PG
SO4	SULFATE ION	O_4S	SO4

Named Sites: **ACT**

h c b g b cg e e cg ge b

CATH: **Structural Classification**
PDBSum: **Summary of PDB Structure**
SCOP: **Structural Classification**

h c b g b cg e e cg ge b

CATH PDB code search

Search results for 1pin

Found 1 related domain

Domain	CATH code	Length	Image
1pinA0	3.40.940.10	*153*	

h b che c c cg b c h ch e e

1pin Chain A Summary page

COMPLEX ISOMERASE/DIPEPTIDE MOL_ID: 1; MOL_ID: 1;

Sequence:

KLPPGWEKRMSRSSGRVYYFNHITNASQWERPSGGKNGQGEPARVRCSHLLVKHSQSRRPSSWRQEKITR
TKEEALELINGYIQKIKSGEEDFESLASQFSDCSSAKARGDLGAFSRGQMQKPFEDASFALRTGEMSGPV
FTDSGIHIILRTE

Number of residues is: 153

Percentage of strand is: 22.9 Percentage of alpha helix is: 22.2 Percentage of 3,10 helix is: 3.3

Secondary Structure Summary:

TETETEETTHHGETHTEE

SHEETS

Number strands	Name	Type	Barrel	Topology
3	A	ANTI	N	1 1
4	B	ANTI	N	-1 3 -1

STRANDS

Location	Sheet
11 - 15	A
22 - 26	A
32 - 33	A
55 - 62	B
121 - 125	B
150 - 151	B
156 - 163	B

B-TURNS

Location	Seq	Type
52 - 55	PARV	VIII
64 - 67	HSQS	I
67 - 70	SRRP	VIII
72 - 75	SWRQ	I
75 - 78	QEKI	VIII
99 - 102	GEED	VIII
118 - 121	ARGD	I'
126 - 129	SRGQ	II
142 - 145	RTGE	II
152 - 155	TDSG	I

HAIRPINS

Location	Class
11 - 26	4: 6
22 - 33	4: 6
55 - 125	60: 62
150 - 163	2: 4

HELICES

Location	Type
82 - 98	H
103 - 110	H
114 - 118	G
132 - 140	H

G-TURNS

Location	Seq	Type
69 - 71	RPS	INV

B-TURNS

Location	Seq	Type
8 - 11	PPGW	II
16 - 19	SRSS	II
26 - 29	NHIT	I
27 - 30	HITN	I
46 - 49	KNGQ	IV

BULGES

Location	Type	Seq
A 26 A 30 A 31	A G	NNA
A 57 A 122 A 123	A C	CLG
A 56 A 162 A 163	A C	RTE

h b che c c b b b h

PDBsum

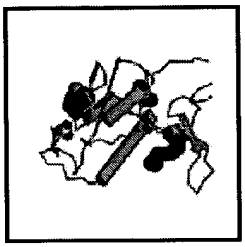

PDB id: 1pin

Complex (isomerase/dipeptide)

Title: *Pin1 peptidyl-prolyl cis-trans isomerase from homo sapiens*

Structure: *Peptidyl-prolyl cis-trans isomerase. Chain: a. Synonym: pin1. Engineered: yes. Ala-pro dipeptide. Chain: b. Engineered: yes*
Source: *Homo sapiens. Human. Cell_line: hela cell. Gene: pin1. Expressed in: escherichia coli. Other_details: using the human gene, the protein was overexpressed in escherichia coli. Synthetic: yes*

RasMol

VRML v.1.0

Structure viewers HELP!

Resolution: 1.35Å. **R-factor:** 0.223. **R-free:** 0.266.

Authors: J.P.Noel, R.Ranganathan, T.Hunter

Date: 21-Jun-98

PDB header records

SWISS-PROT code: PIN1_HUMAN Swiss-prot Pfam

Enzyme class from PDB file: **E.C.5.2.1.8** E.C.->PDB

Molecule(s) in PDB file 1pin:

- **Chain A** (**153** residues)
  - CATH structural classification (1 domain) :

Links	CATH no.	Class	Architecture

h b che c c b b h

CATH DHS **3.40.940.10** -> *Alpha Beta 3-Layer(aba) Sandwich*

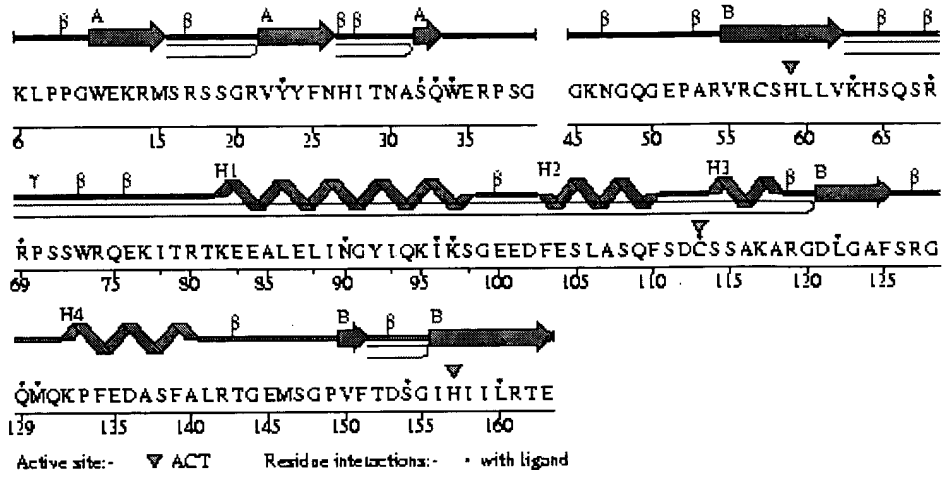

Postscript version

View chain **A** alone.

- **PROMOTIF** summary :
  2 sheets, 7 strands, 4 helices, 15 beta turns, 1 gamma turn, 3 beta bulges, 4 beta hairpins.
- **Active site:** ▽ ACT
- **TOPS** protein topology cartoon
- SAS - annotated FASTA alignment of related sequences in the **PDB**
- **PROSITE** patterns present in this chain:- HELP!

  1. **PS01096 - PPIC_PPIASE.**
     ☐ Phe103->Gly123: **FESLASQFSDCSSAKARGDLG**
  2. **PS01159 - WW_DOMAIN_1.**
     ☐ Trp11->Pro37: **WEKRMSRSSGRVYYFNHITNASQWERP**

  Use the check-boxes to select pattern(s) to view on the 3D structure in **RasMol**, and press:
  DISPLAY
- **MolScript** picture (PostScript file)

● *Ligand:* **ALA-PRO** (**2** residues)

- Schematic diagram of molecule
- Raster3D picture of molecule
- LIGPLOT of interactions

h b che c c b b h

- **2 x** *Ligand:* **1PG** - *Representative polyethylene glycol fragment* Formula: **2(C11 H24 O6)**
  - Schematic diagram of molecule
  - Raster3D picture of molecule
  - LIGPLOT of interactions

- *Ligand:* **SO4** - *Sulfate ion* Formula: **O4 S1 2-**
  - Schematic diagram of molecule
  - Raster3D picture of molecule
  - LIGPLOT of interactions

- **204** water molecules.

PDBsum

h b che c c b b h

```
HEADER    COMPLEX (ISOMERASE/DIPEPTIDE)          21-JUN-98   1PIN
TITLE     PIN1 PEPTIDYL-PROLYL CIS-TRANS ISOMERASE FROM HOMO SAPIENS
COMPND    MOL_ID: 1;
COMPND   2 MOLECULE: PEPTIDYL-PROLYL CIS-TRANS ISOMERASE;
COMPND   3 CHAIN: A;
COMPND   4 SYNONYM: PIN1;
COMPND   5 EC: 5.2.1.8;
COMPND   6 ENGINEERED: YES;
COMPND   7 MOL_ID: 2;
COMPND   8 MOLECULE: ALA-PRO DIPEPTIDE;
COMPND   9 CHAIN: B;
COMPND  10 ENGINEERED: YES
SOURCE    MOL_ID: 1;
SOURCE   2 ORGANISM_SCIENTIFIC: HOMO SAPIENS;
SOURCE   3 ORGANISM_COMMON: HUMAN;
SOURCE   4 CELL_LINE: HELA CELL;
SOURCE   5 GENE: PIN1;
SOURCE   6 EXPRESSION_SYSTEM: ESCHERICHIA COLI;
SOURCE   7 EXPRESSION_SYSTEM_STRAIN: BL21 (DE3);
SOURCE   8 EXPRESSION_SYSTEM_CELLULAR_LOCATION: CYTOPLASM;
SOURCE   9 EXPRESSION_SYSTEM_VECTOR_TYPE: PLASMID;
SOURCE  10 EXPRESSION_SYSTEM_PLASMID: PET28A(+);
SOURCE  11 OTHER_DETAILS: USING THE HUMAN GENE, THE PROTEIN WAS
SOURCE  12 OVEREXPRESSED IN ESCHERICHIA COLI;
SOURCE  13 MOL_ID: 2;
SOURCE  14 SYNTHETIC: YES
KEYWDS    PEPTIDYL-PROLYL CIS-TRANS ISOMERASE, ROTAMASE,
KEYWDS   2 COMPLEX (ISOMERASE/DIPEPTIDE)
EXPDTA    X-RAY DIFFRACTION
AUTHOR    J.P.NOEL,R.RANGANATHAN,T.HUNTER
REVDAT   2   25-NOV-98 1PINA    3       HET    COMPND REMARK TITLE
REVDAT   2 2                     3       HETATM SEQADV HEADER SOURCE
REVDAT   2 3                     3       SEQRES FORMUL KEYWDS CONECT
REVDAT   2 4                     3       HETNAM
REVDAT   1   14-OCT-98 1PIN     0
JRNL        AUTH   R.RANGANATHAN,K.P.LU,T.HUNTER,J.P.NOEL
JRNL        TITL   STRUCTURAL AND FUNCTIONAL ANALYSIS OF THE MITOTIC
JRNL        TITL 2 ROTAMASE PIN1 SUGGESTS SUBSTRATE RECOGNITION IS
JRNL        TITL 3 PHOSPHORYLATION DEPENDENT
JRNL        REF    CELL(CAMBRIDGE,MASS.)           V.  89   875 1997
JRNL        REFN   ASTM CELLB5  US ISSN 0092-8674                  0998
REMARK   1
REMARK   1 REFERENCE 1
REMARK   1  AUTH   K.P.LU,S.D.HANES,T.HUNTER
REMARK   1  TITL   A HUMAN PEPTIDYL-PROLYL ISOMERASE ESSENTIAL FOR
REMARK   1  TITL 2 REGULATION OF MITOSIS
REMARK   1  REF    NATURE                          V. 380   544 1996
REMARK   1  REFN   ASTM NATUAS  UK ISSN 0028-0836                  0006
REMARK   2
REMARK   2 RESOLUTION. 1.35 ANGSTROMS.
REMARK   3
REMARK   3 REFINEMENT.
REMARK   3   PROGRAM     : X-PLOR 3.851
REMARK   3   AUTHORS     : BRUNGER
REMARK   3
REMARK   3  DATA USED IN REFINEMENT.
REMARK   3   RESOLUTION RANGE HIGH (ANGSTROMS) : 1.35
REMARK   3   RESOLUTION RANGE LOW  (ANGSTROMS) : 6.00
REMARK   3   DATA CUTOFF            (SIGMA(F)) : 0
REMARK   3   DATA CUTOFF HIGH         (ABS(F)) : 1000000
```

h b che c c cg b c h e b

```
REMARK   3   DATA CUTOFF LOW          (ABS(F)) : 0.1
REMARK   3   COMPLETENESS (WORKING+TEST)   (%) : 95
REMARK   3   NUMBER OF REFLECTIONS             : 31532
REMARK   3
REMARK   3  FIT TO DATA USED IN REFINEMENT.
REMARK   3   CROSS-VALIDATION METHOD           : THROUGHOUT
REMARK   3   FREE R VALUE TEST SET SELECTION   : RANDOM
REMARK   3   R VALUE            (WORKING SET) : 0.223
REMARK   3   FREE R VALUE                      : 0.266
REMARK   3   FREE R VALUE TEST SET SIZE   (%) : 5
REMARK   3   FREE R VALUE TEST SET COUNT       : 1678
REMARK   3   ESTIMATED ERROR OF FREE R VALUE   : 0.01
REMARK   3
REMARK   3  FIT IN THE HIGHEST RESOLUTION BIN.
REMARK   3   TOTAL NUMBER OF BINS USED           : 12
REMARK   3   BIN RESOLUTION RANGE HIGH       (A) : 1.35
REMARK   3   BIN RESOLUTION RANGE LOW        (A) : 1.39
REMARK   3   BIN COMPLETENESS (WORKING+TEST) (%) : 69
REMARK   3   REFLECTIONS IN BIN    (WORKING SET) : 2054
REMARK   3   BIN R VALUE           (WORKING SET) : 0.377
REMARK   3   BIN FREE R VALUE                    : 0.372
REMARK   3   BIN FREE R VALUE TEST SET SIZE  (%) : 5
REMARK   3   BIN FREE R VALUE TEST SET COUNT     : 106
REMARK   3   ESTIMATED ERROR OF BIN FREE R VALUE : 0.05
REMARK   3
REMARK   3  NUMBER OF NON-HYDROGEN ATOMS USED IN REFINEMENT.
REMARK   3   PROTEIN ATOMS            : 1214
REMARK   3   NUCLEIC ACID ATOMS       : 0
REMARK   3   HETEROGEN ATOMS          : 41
REMARK   3   SOLVENT ATOMS            : 204
REMARK   3
REMARK   3  B VALUES.
REMARK   3   FROM WILSON PLOT           (A**2) : NULL
REMARK   3   MEAN B VALUE      (OVERALL, A**2) : 20
REMARK   3   OVERALL ANISOTROPIC B VALUE.
REMARK   3    B11 (A**2) : NULL
REMARK   3    B22 (A**2) : NULL
REMARK   3    B33 (A**2) : NULL
REMARK   3    B12 (A**2) : NULL
REMARK   3    B13 (A**2) : NULL
REMARK   3    B23 (A**2) : NULL
REMARK   3
REMARK   3  ESTIMATED COORDINATE ERROR.
REMARK   3   ESD FROM LUZZATI PLOT        (A) : NULL
REMARK   3   ESD FROM SIGMAA              (A) : NULL
REMARK   3   LOW RESOLUTION CUTOFF        (A) : NULL
REMARK   3
REMARK   3  CROSS-VALIDATED ESTIMATED COORDINATE ERROR.
REMARK   3   ESD FROM C-V LUZZATI PLOT    (A) : NULL
REMARK   3   ESD FROM C-V SIGMAA          (A) : NULL
REMARK   3
REMARK   3  RMS DEVIATIONS FROM IDEAL VALUES.
REMARK   3   BOND LENGTHS                 (A) : 0.008
REMARK   3   BOND ANGLES            (DEGREES) : 1.78
REMARK   3   DIHEDRAL ANGLES        (DEGREES) : NULL
REMARK   3   IMPROPER ANGLES        (DEGREES) : 1.27
REMARK   3
REMARK   3  ISOTROPIC THERMAL MODEL : RESTRAINED
REMARK   3
REMARK   3  ISOTROPIC THERMAL FACTOR RESTRAINTS.    RMS    SIGMA
```

h b che c c cg b c h e b

```
REMARK   3   MAIN-CHAIN BOND              (A**2) : 1.0   ; 2.0
REMARK   3   MAIN-CHAIN ANGLE             (A**2) : 1.5   ; 1.5
REMARK   3   SIDE-CHAIN BOND              (A**2) : 2.0   ; 2.5
REMARK   3   SIDE-CHAIN ANGLE             (A**2) : 2.0   ; 2.0
REMARK   3
REMARK   3  NCS MODEL : NULL
REMARK   3
REMARK   3  NCS RESTRAINTS.                              RMS   SIGMA/WEIGHT
REMARK   3   GROUP  1  POSITIONAL                (A) : NULL  ; NULL
REMARK   3   GROUP  1  B-FACTOR                (A**2) : NULL  ; NULL
REMARK   3
REMARK   3  PARAMETER FILE  1  : PARAM19X.PRO
REMARK   3  PARAMETER FILE  2  : PARHCSDX.PRO
REMARK   3  TOPOLOGY FILE  1   : TOPH19X.PRO
REMARK   3  TOPOLOGY FILE  2   : TOPHCSDX.PRO
REMARK   3
REMARK   3  OTHER REFINEMENT REMARKS: NULL
REMARK   4
REMARK   4 1PIN COMPLIES WITH FORMAT V. 2.2, 16-DEC-1996
REMARK   6
REMARK   6 RESIDUES  1 - 5 AND 40 - 44 (WHICH LINK THE WW DOMAIN TO
REMARK   6 THE PPIASE DOMAIN) WERE NOT VISIBLE IN THE FINAL ELECTRON
REMARK   6 DENSITY MAP AND SO WERE NOT MODELLED.
REMARK 200
REMARK 200 EXPERIMENTAL DETAILS
REMARK 200  EXPERIMENT TYPE                : X-RAY DIFFRACTION
REMARK 200  DATE OF DATA COLLECTION        : MAR-1996
REMARK 200  TEMPERATURE           (KELVIN) : 100
REMARK 200  PH                             : 7.5
REMARK 200  NUMBER OF CRYSTALS USED        : 1
REMARK 200
REMARK 200  SYNCHROTRON              (Y/N) : Y
REMARK 200  RADIATION SOURCE               : SSRL
REMARK 200  BEAMLINE                       : 7-1
REMARK 200  X-RAY GENERATOR MODEL          : NULL
REMARK 200  MONOCHROMATIC OR LAUE    (M/L) : M
REMARK 200  WAVELENGTH OR RANGE        (A) : 1.08
REMARK 200  MONOCHROMATOR                  : NULL
REMARK 200  OPTICS                         : NULL
REMARK 200
REMARK 200  DETECTOR TYPE                  : IMAGE PLATE
REMARK 200  DETECTOR MANUFACTURER          : MARRESEARCH
REMARK 200  INTENSITY-INTEGRATION SOFTWARE : DENZO
REMARK 200  DATA SCALING SOFTWARE          : SCALEPACK
REMARK 200
REMARK 200  NUMBER OF UNIQUE REFLECTIONS   : 33672
REMARK 200  RESOLUTION RANGE HIGH      (A) : 1.35
REMARK 200  RESOLUTION RANGE LOW       (A) : 25.0
REMARK 200  REJECTION CRITERIA  (SIGMA(I)) : NONE
REMARK 200
REMARK 200 OVERALL.
REMARK 200  COMPLETENESS FOR RANGE     (%) : 95.5
REMARK 200  DATA REDUNDANCY                : 4.5
REMARK 200  R MERGE                    (I) : NULL
REMARK 200  R SYM                      (I) : 0.053
REMARK 200   FOR THE DATA SET  : 18
REMARK 200
REMARK 200 IN THE HIGHEST RESOLUTION SHELL.
REMARK 200  HIGHEST RESOLUTION SHELL, RANGE HIGH (A) : 1.35
REMARK 200  HIGHEST RESOLUTION SHELL, RANGE LOW  (A) : 1.39
```

h b che c c cg b c h e b

UPF2 and *UPF3* genes[13,15–17]. Finally, the *MRT1* and *MRT3* gene products, which are only required for deadenylation-dependent decapping[7], appear to promote decapping following deadenylation. These proteins may all directly affect the interaction of the decapping enzyme with each mRNA. Alternatively, modulation of decapping rate may occur by alterations in mRNP structure that affect the accessibility of the cap structure to the decapping enzyme. For example, control of decapping rate may occur through competition for the 5′ cap structure between the eIF-4F cap binding complex and the decapping enzyme. Such a model is appealing in that it would provide a mechanistic basis for the observation that the translation and turnover of eukaryotic mRNAs are often coupled. □

Received 9 February; accepted 20 June 1996.

1. Decker, C. J. & Parker, R. *Genes Dev.* **7,** 1632–1643 (1993).
2. Hsu, C. L. & Stevens, A. *Molec. cell. Biol.* **13,** 4826–4835 (1993).
3. Muhlad, D., Decker, C. J. & Parker, R. *Genes Dev.* **8,** 855–866 (1994).
4. Muhlrad, D., Decker, C. J. & Parker, R. *Molec. cell. Biol.* **15,** 2145–2156 (1995).
5. Muhlrad, D. & Parker, R. *Genes Dev.* **6,** 2100–2111 (1992).
6. Muhlrad, D. & Parker, R. *Nature* **370,** 578–581 (1994).
7. Hatfield, L., Beelman, C. A., Stevens, A. & Parker, R. *Molec. cell. Biol.* (in the press).
8. Stevens, A. *Molec. cell. Biol.* **8,** 2005–2010 (1988).
9. Hochuli, E., Döbeli, H. & Schacher, A. *J. Chromatogr.* **411,** 177–184 (1987).
10. Beelman, C. A. & Parker, R. *Cell* **81,** 179–183 (1995).
11. Decker, C. J. & Parker, R. *Trends biochem. Sci.* **19,** 336–340 (1994).
12. Peltz, S. W., He, F., Welch, E. & Jacobson, A. *Prog. Nucleic Acids Res. molec. Biol.* **17,** 271–298 (1994).
13. He, F. & Jacobson, A. *Genes Dev.* **9,** 437–454 (1995).
14. Caponigro, G. & Parker, R. *Genes Dev.* **9,** 2421–2432 (1995).
15. Leeds, P., Peltz, S. W., Jacobson, A. & Culbertson, M. R. *Genes Dev.* **5,** 2303–2314 (1991).
16. Leeds, P., Wood, J. M., Lee, B.-S. & Culbertson, M. R. *Molec. cell. Biol.* **12,** 2165–2177 (1992).
17. Cui, Y., Hagan, K. W., Zhang, S. & Peltz, S. W. *Genes Dev.* **9,** 423–436 (1995).
18. Johnson, A. W. & Kolodner, R. D. *J. biol. Chem.* **266,** 14046–14054 (1991).
19. Mandart, E. & Parker, R. *Molec. cell. Biol.* **15,** 6979–6986 (1995).
20. Harris, M. E. *et al. EMBO J.* **13,** 3953–3963 (1994).
21. Caponigro, G., Muhlrad, D. & Parker, R. *Molec. cell. Biol.* **13,** 5141–5148 (1993).

ACKNOWLEDGEMENTS. We thank members of R.P.'s laboratory for comments on the manuscript and S. Peltz for technical suggestions on the decapping assay. The NH_2-terminal sequencing of the purified decapping enzyme was done by the City of Hope Microsequencing and Mass Spectrometry Core Facility, Beckman Research Institute of City of Hope, Duarte, California. This work was supported by grants from the NIH to R.P. and funds from the HHMI. A.S. was supported by the Office of Health and Environmental Research, US Department of Energy, under contract with the Lockheed Martin Energy Systems, Inc.

SUPPLEMENTARY INFORMATION is available on *Nature*'s World-Wide Web site (http://www.nature.com). Paper copies are available from Mary Sheehan at the London editorial office of *Nature*.

CORRESPONDENCE and requests for materials should be addressed to R.P. (e-mail: parker_lab@tikal.biosci.arizona.edu).

Structure of the WW domain of a kinase-associated protein complexed with a proline-rich peptide

Maria J. Macias, Marko Hyvönen, Elena Baraldi, Johan Schultz*, Marius Sudol†, Matti Saraste & Hartmut Oschkinat

European Molecular Biology Laboratory, Meyerhofstrasse 1, 69117 Heidelberg, Germany
* Forschungsinstitut für Molekulare Pharmakologie, Alfred-Kowalke-Str. 4, 10315 Berlin, Germany
† Mount Sinai School of Medicine, Department of Biochemistry, Box 1020, One Gustave L. Levy Place, New York, New York 10029-6574, USA

THE WW domain is a new protein module with two highly conserved tryptophans that binds proline-rich peptide motifs *in vitro*. It is present in a number of signalling and regulatory proteins, often in several copies[1–3]. Here we investigate the solution structure of the WW domain of human YAP65 (for Yes kinase-associated protein) in complex with proline-rich peptides containing the core motif PPxY (ref. 4). The structure of the domain with the bound peptide GTPPPPYTVG is a slightly curved, three-stranded, antiparallel β-sheet. Two prolines pack against the first tryptophan, forming a hydrophobic buckle on the convex side of the sheet. The concave side has three exposed hydrophobic residues (tyrosine, tryptophan and leucine) which form the binding site for the ligand. A non-conserved isoleucine in the amino-terminal flanking region covers a hydrophobic patch and stabilizes the WW domain of human YAP65 *in vitro*. The structure of the WW domain differs from that of the SH3 domain and reveals a new design for a protein module that uses stacked aromatic surface residues to arrange a binding site for proline-rich peptides.

The WW domain forms a new family of protein modules[1–3], analogous to the Src-homology-2 and -3 (SH2, SH3), pleckstrin-homology (PH) and phosphotyrosine-binding (PTB) domains[5–9]. It consists of ~38 amino acids[1] with a high content of hydrophobic, aromatic and proline residues (Fig. 1), and two highly conserved tryptophans (hence WW domain). Like other intracellular protein modules, the WW domain is present in a variety of cytoskeletal and signal-transducing proteins, such as YAP65, dystrophin, ubiquitin-protein ligases, the transcriptional activator FE65 and proteins binding to formin[1–3,10]. It binds proline-rich peptides, as do SH3 domains[11,12], and WW and SH3 domains may compete for binding to the same sequence motifs[10]. The WW domain of human YAP (hYAP) binds peptides with a consensus sequence PPxY *in vitro*[4]. A WW domain is necessary for control of epithelial sodium channels: carboxy-terminal deletions of the amiloride-sensitive channel cause Liddle's syndrome, a hereditary form of hypertension. The C terminus contains PPxY motifs that interact with a WW domain in the regulatory protein Nedd4 (refs 13, 14), indicating that WW domains may be alternative recognition sites for proline-rich ligands.

Several constructs of the WW domain hYAP with variable N- and C-terminal extensions were made and expressed in *Escherichia coli*. Although intact fusion proteins with glutathione-*S*-transferase (GST) were always obtained, only two could be purified after cleavage with thrombin (Fig. 1, bottom). Construct 1 was folded, as indicated by a number of amide proton signals between 8.5 and 9.5 p.p.m. in the ^{1}HNMR spectrum. From the multiple sequence alignment (Fig. 1), construct 2 should already contain the full-length domain, but its NMR spectrum did not show any amide resonances with chemical shifts larger than 8.5 p.p.m., the signals of the aromatic residues were not dispersed, and the two-dimensional spectra gave a peak pattern typical of a random coil. We therefore used construct 1 in all further experiments, which was also labelled with ^{13}C and ^{15}N.

We determined the structure of the hYAP WW domain in a complex with the proline-rich peptide GTPPPPYTVG. The domain structure consists of a twisted and slightly bent three-stranded antiparallel β-sheet (Fig. 2*a*) comprising residues 16–22, 26–32 and 35–39. It is well ordered in the region L13–P42 (Fig. 2*b* and Table 1), where residues 14–17, 23–25, 33–34 and 40–42 form well defined turns. Residues Y28 and W39 are located on the bottom side, and F29 and W17 are on the top side of the sheet (Fig. 2*b*). The side chains of Y28 and W39 fill its concave side so that an almost flat hydrophobic surface is produced. The N and C termini of the domain meet on the convex side to form a hydrophobic buckle, in which the side chains of P14 and P42 are positioned opposite each other above W17.

The stretches comprising residues 1–6, 8–12, and 43–50 show only few weak long- or medium-range nuclear Overhauser effects (NOEs) (11 → 43, 43 → 45) and appear to be flexible. The core domain as defined by the sequence alignment has an exposed hydrophobic surface in the front of the buckle. This is covered by isoleucine at position 7 (red in Fig. 2*b*) like a snap fastener, with

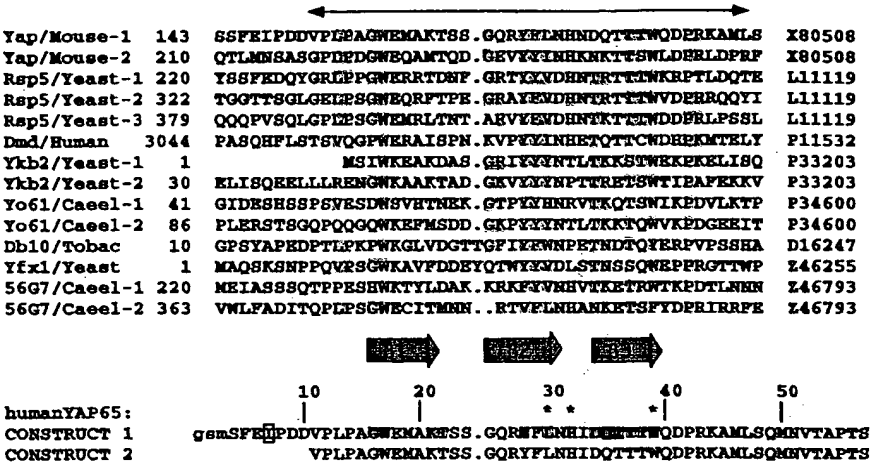

FIG. 1 Sequence alignment of WW domains from selected proteins. Residue numbers are shown on the left, and accession numbers on the right. Bottom, constructs 1 and 2 of the WW domain from human YAP65; residue numbering is based on construct 1. Residues showing strong chemical shift changes upon peptide binding (>0.5 p.p.m.) are indicated in red; those showing smaller changes (0.2 p.p.m.) are labelled in blue. Residues with a star above the sequence of construct 1 show NOEs to the ligand peptide. The isoleucine residue at position 7 that is essential for folding is in an open box. The domain boundaries originally proposed[1] are indicated by an arrow.

METHODS. Both constructs were amplified by using the polymerase chain reaction (PCR) and cloned human YAP65 cDNA as template. Amplified fragments were cloned into GST fusion vector pGAT2 (J. Peränen and M.H., unpublished). The expressed fusion protein contains both a His-tag and GST, allowing double-affinity purification. The WW domain was released from the fusion protein by thrombin. All DNA constructs were verified by dideoxy sequencing. Proteins were expressed in the *E. coli* strain BL21(DE3) and purified by affinity chromatography on glutathione–Sepharose (Pharmacia), Ni^{2+}-NTA-agarose (QIAGEN), and gel filtration on a Superdex-30 (Pharmacia) column (details of purification available on request). Relative molecular masses of purified proteins were determined by electrospray mass spectrometry. The three mutants were made by PCR mutagenesis using construct 1 as a template; they were cloned and expressed as the wild-type protein.

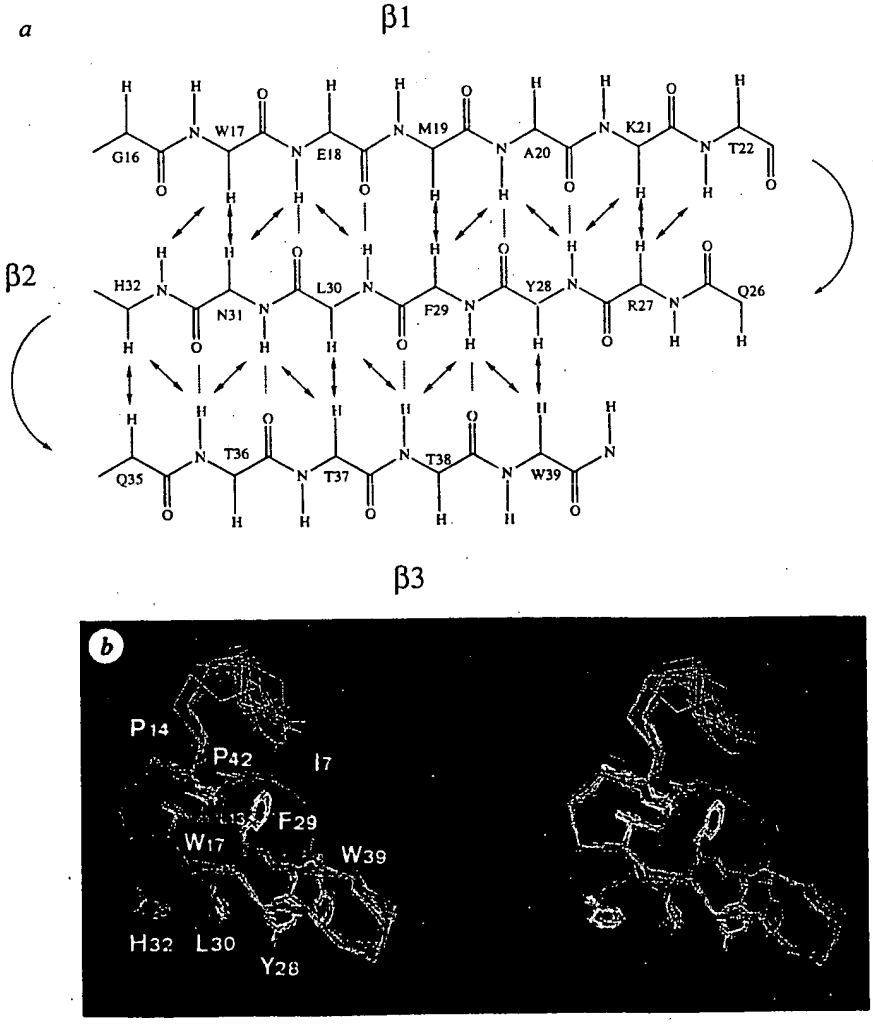

FIG. 2 *a*, Secondary structure NOE pattern of the WW domain. Hydrogen bonds are indicated by dotted lines if the predicted interstrand NOEs are present. Series of COSY, NOESY and clean TOCSY[18–20] spectra of an unlabelled construct 1 with and without the peptide ligand (protein concentration 1.2 mM, peptide:protein ratio 3:1, 10 mM potassium phosphate, pH 6, 100 mM NaCl, 0.1 mM DTT, 0.1 mM EDTA, 0.02% NaN_3) were recorded at 600 MHz and 285 K and 278 K, leading to nearly complete assignments. HCCH-TOCSY[21] and 3D ^{13}C-resolved NOESY[22,23] spectra were measured using [^{13}C, ^{15}N]-labelled protein and unlabelled peptide. Various $^{13}C/^{12}C$-filtered spectra[24] were used to differentiate between intermolecular and intramolecular NOEs and to assign signals from the bound peptide. Owing to the broadness of the signals in the environments of the bound peptide and P42 (residue numbering refers to construct 1; Fig. 1), a NOESY spectrum was recorded at 750 MHz in D_2O. This yielded sharper lines and therefore additional NOEs, especially between P14 and P42, and between the WW domain and the bound peptide. *b*, Superposition of 13 structures with the lowest energy, showing the backbone of residues I7–P42 and the side chains of I7, P14, W17, Y28, F29, L30, H32, I33, W39 and P42. The side chain of I7 that is necessary for the folding of the domain is shown red, all others are yellow. The structures were calculated using a standard simulated annealing protocol[15] and X-PLOR[16]. For structure statistics, see Table 1.

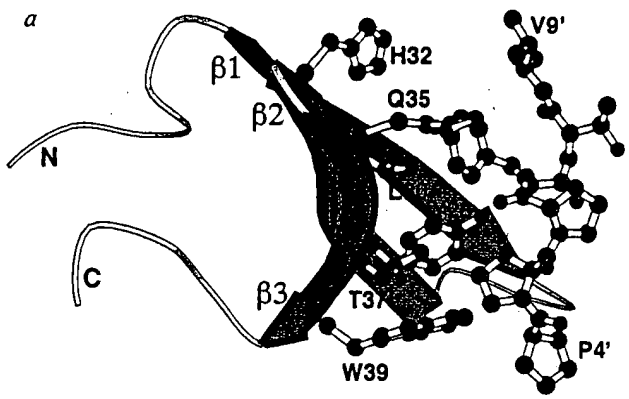

FIG. 3 *a*, A model of the peptide/WW-domain complex drawn with MOLSCRIPT[25]. Only the residues of the peptide showing contacts to the protein are shown (P4′–V9′). The peptide was modelled by using ten intermolecular NOEs and restraining the conformation of the proline segment into a polyproline type II polyproline. The side chains of the domain (carbon atoms in black) and ligand (in green) residues that are involved in the interaction are shown. Nitrogen atoms are blue, oxygen atoms red. *b*, *c*, The model of the complex drawn with GRASP[26] shows the van der Waals surface of the WW domain and the bound peptide ligand as a stick presentation.

contacts to F29, P14 and P42. This residue is outside the domain core and may be uniquely important for the stability of the hYAP WW domain as it is not conserved in the N-terminal flanking region (Fig. 1).

As the consensus of the hYAP WW ligand is PPxY (ref. 4), we used two peptides for structural studies (GTPPPPYTVG and SPPPYTV) that had this sequence at residues 4′–7′ and 2′–5′, respectively (peptide residues are primed). The binding site for both peptides, as indicated by chemical shift changes (Fig. 1) and peptide-protein NOEs, corresponds to the area that is defined by residues Y28, L30, H32 and six residues from D34 to W39 on the concave side of the domain. This area presents a large hydrophobic patch on the protein surface formed by the side chains of Y28, L30, W39 and a number of threonine methyl groups. The pattern of intermolecular NOEs is formed by contacts between the ligand residues P5′ and W39, Y7′ and L30 and H32, and V9′

TABLE 1 Structure statistics and binding constants of complexes

Structure statistics	
Number of constraints	
sequential	160
medium-range	87
long-range	219
intramolecular	30
hydrogen-bond mimics (2 NOEs each)	8
intermolecular	10
Number of NOEs per residue (13–43)	15
X-PLOR potential energy (kcal m^{-1})	
E_{total}	184 ± 5
E_{bonds}	13 ± 1
E_{angles}	92 ± 4
$E_{impropers}$	7 ± 2
E_{vdW}	17 ± 3
E_{NOE}	44 ± 2
R.m.s.d. from ideal values	
angles	0.60 ± 0.02
impropers	0.41 ± 0.02

R.m.s.d. (Å) between average ⟨$\overline{SA}$⟩ and selected set of structures ⟨SA⟩ for residues 13–43

	Backbone	All heavy
⟨SA⟩ versus ⟨SA⟩	0.54 ± 0.20	0.90 ± 0.20

Binding constants of mutant proteins and peptides

Protein	Peptide	Binding constant (μM)
WT	SPPPYTV	47 ± 6
WT	GTPPPPYTVG	52 ± 6
L30K	SPPPYTV	n.b.
L30K	GTPPPPYTVG	40 ± 5*
H32A	SPPPYTV	n.b.
H32A	GTPPPPYTVG	n.b.
Q35A	SPPPYTV	n.b.
Q35A	GTPPPPYTVG	160 ± 18
WT	SPPPPATV	n.b.
WT	SPPPPLTV	n.b.
WT	SPPPPFTV	118 ± 17
WT	SAPPPYTV	53 ± 17
WT	SPAPPYTV	n.b.
WT	SPPAPYTV	n.b.
WT	SPPPAYTV	63 ± 17

SA, simulated annealing; WT, wild type; n.b., no binding observed by fluorescence spectroscopy. Dissociation constants were determined by changes in the fluorescence emission spectra of our WW construct 1 upon addition of peptide at defined concentrations; calculations were made assuming formation of a 1:1 complex[17]. Fluorescence was measured at 25 °C in an Aminco Bowmann series-2 luminescence spectrophotometer. Excitation wavelength was 298 nm, using a slit width of 2 nm. Fluorescence spectra were recorded from 310 to 360 nm wavelength, using a slit width of 4 nm. The protein concentration was kept at 10 μM in a 40 mM phosphate buffer at pH 7.2.

* This value does not agree with the other data and must be due to a structural rearrangement.

and H32. The NOEs clearly define the orientation of the ligand peptide on the WW domain.

The proline-containing part of peptide GTPPPPYTVG was restrained into a polyproline helix type II, and the structure of the complex was calculated using a standard simulated annealing protocol[15] (X-PLOR[16]) and the ten intermolecular NOEs as constraints. The result shows smooth contacts between the ligand and the domain (Fig. 3). The central prolines P4′ and P5′ contact W39, and the carbonyl group of P6′ points towards the OH group of the conserved residue Y28. The peptide tyrosyl residue Y7′ is accommodated in a hydrophobic pocket formed by L30 and H32. These contacts are well defined by six NOEs between the aromatic ring of Y7′ and the side chains of L30 and H32. Y7′ could form a hydrogen bond to the histidine ring but also to Q35, whose chemical shifts change strongly on peptide binding (Fig. 1).

The aromatic residues at positions 39 and 28, a hydrophobic residue at position 30 and a histidine at position 32 all tend to be conserved (Fig. 1). Our structure shows that these are the residues that are in contact with the peptide. The importance of this hydrophobic surface is underscored by the low binding affinity of mutants H32A, L30K and Q35A to both peptides (except in one case, see Table 1; E.B. *et al.*, unpublished results). The structure of the mutants remained intact, as judged by their two-dimensional NMR spectra. The binding affinities of peptides in which the tyrosine residue of SPPPPYTV is substituted with alanine, leucine or phenylalanine show that the YAP domain is specific for a tyrosine-containing motif. In the first two cases there is no binding, and the peptide containing phenylalanine has only a weak affinity (Table 1). Thus, the tyrosine in the PPxY motif may be needed for the interaction of ligands with a set of WW domains. The importance of the polyproline motif is shown by the lack of binding when the two centre prolines in this peptide are replaced by alanines, whereas replacement of the first proline has no effect (Table 1).

Our structure confirms the hypothesis[4] that the WW domain is a binding module for proline-rich ligands. The PPxY motif may not be the only ligand for WW domains: for instance, it is not present in the proline-rich tail of formin that interacts with SH3 and WW domains[10], where sequence motifs such as PPxLP are found. The structure indicates that hydrophobic residues replacing tyrosine of the ligand could be accommodated on the surface of those domains that contain hydrophobic residues other than leucine at position 30.

Note added in proof: An involvement of hYAP in retroviral budding through its WW domain was recently suggested[27]. □

Received 17 May; accepted 24 June 1996.

1. Bork, P. & Sudol, M. *Trends biochem. Sci.* **19,** 531–533 (1994).
2. Andre, B. & Springael, J. Y. *Biochem. biophys. Res. Commun.* **205,** 1201–1205 (1994).
3. Hofmann, K. & Bucher, P. *FEBS Lett.* **358,** 153–157 (1995).
4. Chen, H. I. & Sudol, M. *Proc. natn. Acad. Sci. U.S.A.* **92,** 7819–7823 (1995).
5. Pawson, T. *Nature* **373,** 573–580 (1995).
6. Cohen, G. B., Ren, R. & Baltimore, D. *Cell* **80,** 237–248 (1995).
7. Sudol, M., Chen, H. I., Bougeret, C., Einbond, A. & Bork, P. *FEBS Lett.* **369,** 67–71 (1995).
8. Bork, P. & Margolis, B. *Cell* **80,** 693–694 (1995).
9. Zhou, M. M. *et al. Nature* **378,** 587–592 (1995).
10. Chan, D. C., Bedford, M. T. & Leder, P. *EMBO J.* **15,** 1045–1054 (1996).
11. Cicchtti, P., Mayer, B. J., Thiel, G. & Baltimore, D. *Science* **257,** 803–806 (1992).
12. Ren, R., Mayer, B. J., Cicchetti, P. & Baltimore, D. *Science* **259,** 1157–1161 (1993).
13. Staub, O. *et al. EMBO J.* **15,** 2371–2380 (1996).
14. Schild, L. *et al. EMBO J.* **15,** 2381–2387 (1996).
15. Nilges, M., Clore, G. M. & Gronenborn, A. M. *FEBS Lett.* **229,** 317–324 (1988).
16. Brünger, A. T. *X-PLOR 3.1 Manual* (Yale Univ. Press, New Haven, 1992).
17. Viguera, A. R., Arrondo, J. L. R., Musacchio, A., Saraste, M. & Serrano, L. *Biochemistry* **133,** 10925–10933 (1994).
18. Aue, W. P., Bartholdi, E. & Ernst, R. R. *J. chem. Phys.* **64,** 2229–2246 (1976).
19. Griesinger, C., Otting, G., Wüthrich, K. & Ernst, R. R. *J. Am. chem. Soc.* **110,** 7870–7871 (1988).
20. Jeener, J., Meier, B. H., Bachmann, P. & Ernst, R. R. *J. chem. Phys.* **71,** 4546–4553 (1979).
21. Kay, L. E., Ikura, M., Tschudin, R. & Bax, A. *J. magn. Reson.* **89,** 496–514 (1990).
22. Fesik, S. W. & Zuiderweg, E. R. P. *J. magn. Reson.* **87,** 588–593 (1988).
23. Marion, D., Kay, L. E., Sparks, S. W., Torchia, D. A. & Bax, A. *J. Am. chem. Soc.* **111,** 1515–1517 (1989).
24. Otting, G. & Wüthrich, K. *J. magn. Reson.* **85,** 586–594 (1989).
25. Kraulis, P. *J. appl. Crystallogr.* **24,** 946–950 (1991).
26. Nicholls, A., Sharp, K. A. & Honig, B. *Proteins* **11,** 281–296 (1991).
27. Garnier, L., Wills, J. W., Verderame, M. F. & Sudol, M. *Nature* **381,** 744–745 (1996).

ACKNOWLEDGEMENTS. We thank A. Ulrich for her participation in preliminary experiments; P. Bork, Henry I. Chen and M. Wilmanns for discussion; M. Wilmanns for help in preparing figures; R. Jacob for synthesis of peptides; A. Viguera for help with fluorescence measurements; and H. Kessler and C. Schwarz for facilities and help at the Technische Universität, München. M.S. was supported by MDA and HFSPO grants.

CORRESPONDENCE and requests for materials should be addressed to H.O. (e-mail: oschkinat@embl-heidelberg.de).

Crystal structure of a PDZ domain

João H. Morais Cabral*, Carlo Petosa*, Michael J. Sutcliffe†, Sami Raza†, Olwyn Byron*‖, Florence Poy‡, Shirin M. Marfatia§, Athar H. Chishti§ & Robert C. Liddington*

*Departments of Biochemistry, ‖ NCMH and † Chemistry, University of Leicester, Leicester LE1 7RH, UK
‡Dana–Farber Cancer Institute, 44 Binney Street, Boston, Massachusetts 02115, USA
§Laboratory of Tumor Cell Biology, St Elizabeth's Medical Center, Tufts University School of Medicine, 736 Cambridge Street, Boston, Massachusetts 02135, USA

PDZ domains (also known as DHR domains or GLGF repeats) are ~90-residue repeats found in a number of proteins implicated in ion-channel and receptor clustering, and the linking of receptors to effector enzymes[1]. PDZ domains are protein-recognition modules; some recognize proteins containing the consensus carboxy-terminal tripeptide motif S/TXV with high specificity[2–4]. Other PDZ domains form homotypic dimers: the PDZ domain of the neuronal enzyme nitric oxide synthase binds to the PDZ domain of PSD-95, an interaction that has been implicated in its synaptic association[5]. Here we report the crystal structure of the third PDZ domain of the human homologue of the *Drosophila discs-large* tumour-suppressor gene product, DlgA. It consists of a five-stranded antiparallel β-barrel flanked by three α-helices. A groove runs over the surface of the domain, ending in a conserved hydrophobic pocket and a buried arginine; we suggest that this is the binding site for the C-terminal peptide.

The PDZ domain[6] is named after three of the proteins in which the repeats have been described: PSD-95 (postsynaptic density protein, M_r 95K), Dlg (*discs-large* protein) and ZO-1 (zonula occludens-1). These proteins have a conserved structure comprising three tandem PDZ domains, an SH3 domain and a guanylate-kinase-like domain. Other proteins that contain PDZ domains include certain protein kinases and protein tyrosine phosphatases, and neuronal nitric oxide (NO) synthase[1]. These domains appear to be protein-recognition modules analogous to the well characterized SH2 and SH3 domains.

We crystallized a recombinant form of the third PDZ domain (PDZ-3) from human Dlg and solved its structure at 2.8 Å resolution using two heavy-atom derivatives and solvent flattening (Table 1). A complete model for the 96-residue domain has been built; in spite of a large proportion of glycine residues (13%), all of the secondary structure elements and connecting loops are well ordered. The domain is compact and globular, with a diameter of 25–30 Å. β-strands 2–5 form an up-and-down β-barrel and strand β1 crosses over the barrel and hydrogen-bonds to β5; a short α-helix (α1) and its connecting loop cap one end of the barrel; helix α2 caps the other end of the barrel, and a C-terminal helix (α3) packs against the outside of the barrel (Figs. 1*b* and 2). Most of the conserved residues (Fig. 1*a*) are hydrophobic, and form the core of the domain, which is exposed on one face (Figs 2, 3*b*). There are two exceptions: a conserved aspartic acid (D510), which is buried and forms a salt bridge to an arginine (R465); and an asparagine

the MAPK pathway is tyrosine-kinase dependent has not been reported in other cells. This cell-type specificity of signalling pathways is more likely to be a common theme rather than a variation. □

Received 2 November 1995; accepted 29 February 1996.

1. Marshall, C. J. *Curr. Opin. Genet. Dev.* **4,** 82–89 (1994).
2. Seger, R. & Krebs, E. G. *FASEB J.* **9,** 726–735 (1995).
3. Schlessinger, J. & Ullrich, A. *Neuron* **9,** 383–391 (1992).
4. Takata, M. *et al. EMBO J.* **13,** 1341–1349 (1994).
5. van Corven, E. J., Hordijk, P. L., Medema, R. H., Bos, J. L. & Moolenaar, W. H. *Proc. natn. Acad. Sci. U.S.A.* **90,** 1257–1261 (1993).
6. Hawes, B. E., van Biesen, T., Koch, W. J., Luttrell, L. M. & Lefkowitz, R. J. *J. biol. Chem.* **270,** 17148–17153 (1995).
7. Cook, S. J., Rubinfeld, B., Albert, I. & McCormick, F. *EMBO J.* **12,** 3475–3485 (1993).
8. Crespo, P., Xu, N., Simonds, W. F. & Gutkind, J. S. *Nature* **369,** 418–420 (1994).
9. Faure, M., Voyno-Yasenetskaya, T. A. & Bourne, H. R. *J. biol. Chem.* **269,** 7851–7854 (1994).
10. Koch, W. J., Hawes, B. E., Allen, L. F. & Lefkowitz, R. J. *Proc. natn. Acad. Sci. U.S.A.* **91,** 12706–12710 (1994).
11. Matsuda, S. *et al. EMBO J.* **11,** 973–982 (1992).
12. Seger, R. *et al. J. biol. Chem.* **267,** 14373–14381 (1992).
13. Crews, C. M., Alessandrini, A. & Erikson, R. L. *Science* **258,** 478–480 (1992).
14. Zheng, C. F. & Guan, K. L. *J. biol. Chem.* **268,** 11435–11439 (1993).
15. Alessandrini, A., Crews, C. M. & Erikson, R. L. *Proc. natn. Acad. Sci. U.S.A.* **89,** 8200–8204 (1992).
16. Peralta, E. G. *et al. EMBO J.* **6,** 3923–3929 (1987).
17. Taniguchi, T. *et al. J. biol. Chem.* **266,** 15790–15796 (1991).
18. Boulton, T. G. *et al. Science* **249,** 64–67 (1990).
19. Cohen, G. B., Ren, R. & Baltimore, D. *Cell* **80,** 237–248 (1995).
20. Takata, M. & Kurosaki, T. *FEBS Lett.* **374,** 407–411 (1995).
21. Kurosaki, T. *et al. J. exp. Med.* **182,** 1815–1823 (1995).
22. Shiue, L. *et al. Molec. cell. Biol.* **15,** 272–281 (1995).
23. van Biesen, T. *et al. Nature* **376,** 781–784 (1995).
24. Winitz, S. *et al. J. biol. Chem.* **268,** 19196–19199 (1993).
25. Huang, X.-Y., Morielli, A. D. & Peralta, E. G. *Cell* **75,** 1145–1156 (1993).
26. Langhans-Rajasekaran, S. A., Wan, Y. & Huang, X.-Y. *Proc. natn. Acad. Sci. U.S.A.* **92,** 8601–8605 (1995).
27. Lev, S. *et al. Nature* **376,** 737–745 (1995).

ACKNOWLEDGEMENTS. We thank R. Erikson and E. Peralta and their colleagues for cDNA clones, and M. Chao, R. Erikson, M. C. Gershengorn, T. Maack, L. G. Palmer and the members of our laboratory for reading the manuscript. This work was supported by grants from the NSF, the American Heart Association, and by Cornell University Medical College. X-Y.H. is a Cornell Scholar and a Beatrice F. Parvin Investigator of the American Heart Association New York City affiliate.

CORRESPONDENCE and requests for materials should be addressed to X.-Y.H. (e-mail: xyhuang@med.cornell.edu).

A human peptidyl–prolyl isomerase essential for regulation of mitosis

Kun Ping Lu, Steven D. Hanes* & Tony Hunter

Molecular Biology and Virology Laboratory, The Salk Institute, 10010 North Torrey Pines Road, La Jolla, California 92037, USA
* Wadsworth Center, Laboratory of Developmental Genetics, New York State Department of Health, 120 New Scotland Avenue, Albany, New York 12201, USA

THE NIMA kinase is essential for progression through mitosis in *Aspergillus nidulans*[1–6], and there is evidence for a similar pathway in other eukaryotic cells[5–8]. Here we describe the human protein Pin1, a peptidyl–prolyl *cis/trans* isomerase (PPIase) that interacts with NIMA. PPIases are important in protein folding, assembly and/or transport[9–13], but none has so far been shown to be required for cell viability[9–11]. Pin1 is nuclear PPIase containing a WW protein interaction domain, and is structurally and functionally related to Ess1/Ptf1, an essential protein in budding yeast[14,15]. PPIase activity is necessary for Ess1/Pin1 function in yeast. Depletion of Pin1/Ess1 from yeast or HeLa cells induces mitotic arrest, whereas HeLa cells overexpressing Pin1 arrest in the G2 phase of the cell cycle. Pin1 is thus an essential PPIase that regulates mitosis presumably by interacting with NIMA and attenuating its mitosis-promoting activity.

One class of human complementary DNA clones identified in a yeast two-hybrid screen for proteins interacting with NIMA encoded Pin1, a protein of relative molecular mass (M_r) 18,245 (Fig. 1*a*). Northern blotting showed a single ~ 1.0-kilobase (kb) *PIN1* messenger RNA in all human cell lines tested (data not shown). Pin1 is 45% identical to the budding yeast protein Ess1/Ptf1 (refs 14,15), and contains a putative nuclear localization signal and two identifiable domains, an amino-terminal WW domain and a carboxy-terminal PPIase domain (Fig. 1*a*). The WW domain, characterized by two invariant tryptophans, occurs in a variety of unrelated cell-signalling proteins[16]; in Yap the WW domain mediates protein–protein interactions by binding a Pro-rich sequence[17]. Thus the Pin1 WW domain may act as a protein interaction module that confers specificity to its catalytic domain.

The C terminus of Pin1 contains motifs characteristic of the newly discovered parvulin family of PPIases, which share little similarity with either the cyclophilins or the FK506-binding proteins (FKBPs)[12,13] (Fig. 1*a*). Recombinant Pin1 had concentration-dependent PPIase activity (Fig. 1*b*), which, like parvulin[12], was not inhibited by either cyclosporin A or an FK506 analogue (data not shown). Our results confirm that Pin1 belongs to this family of PPIases[12,13]. Previous failure to detect Ess1/Ptf1 PPIase activity[15] might have been due to its high sensitivity to the chymotrypsin used in the assay. With the possible exception of yeast *CPR3*, which is required under restricted conditions[18], no PPIase has yet been found to be essential for growth[9–11]. Here we show that Pin1/Ess1 is required for normal growth.

The striking sequence similarity between Pin1 and Ess1 prompted us to test whether *PIN1* substitutes for *ESS1* in yeast cells. Diploid cells bearing one disrupted copy of *ESS1* were transformed with a *PIN1* expression plasmid or a control vector, followed by tetrad analysis (Fig. 2*a*). As expected[14], tetrads from cells transformed with the control plasmid showed 2:2 segregation for spore viability (viable:inviable). In contrast, ~ 25% of tetrads from *PIN1*-transformed cells showed 4:0 segregation, demonstrating that *PIN1* complements the *ess1*$^-$ mutation in haploid cells. The growth rates of *PIN1*-expressing *ess1*$^-$ cells were similar to those of control cells (Fig. 2*a*). In plasmid shuffle experiments, *PIN1* also complemented the lethal defect in *ess1*$^-$/*ess1*$^-$ diploid cells (data not shown). Thus human *PIN1* substitutes functionally for *ESS1* in both haploid and diploid yeast cells.

To determine whether the PPIase activity of Pin1 is necessary for its essential function, we tested whether PPIase domain mutants complemented *ess1*$^-$ yeast by tetrad analysis. Cells expressing wild-type Pin1 showed 4:0 segregation for spore viability, whereas cells expressing Pin1 with a C-terminal truncation beyond Ser 114 (*PIN1-3′Δ*) or with Ala substitutions in three highly conserved residues (*PIN1-3A*; G155A, H157A, I159A) showed 2:2 segregation, indicating a failure to complement the *ess1*$^-$ mutation (Fig. 2*b*). A plasmid shuffle assay gave similar results (data not shown). Immunoblot analysis showed that Pin1 and Pin1-3′Δ were expressed at similar levels, whereas slightly less Pin1-3A was expressed (data not shown). Neither mutant protein had detectable PPIase activity when assayed *in vitro* (Fig. 2*b*). These results demonstrate that Pin1/Ess1 PPIase activity is required for cell growth.

To determine the cell-cycle function of *PIN1/ESS1* in yeast, we constructed a haploid *ess1*$^-$ strain that expressed *PIN1* under control of the *GAL1* promoter (*GAL1–PIN1*). Regulated expression of Pin1 was confirmed by immunoblotting (data not shown). As expected, this *PIN1*-dependent strain grew normally in inducing or partial-inducing medium but did not grow in repressing medium. Cells depleted of Pin1 displayed a striking terminal phenotype: mitotic arrest followed by nuclear fragmentation. Cell division slowed 6 hours after shifting from inducing to repressing medium, and by 12 hours cells accumulated in the M phase with 2*n* DNA content and a large bud (Fig. 2*c*). Most cells contained nuclei stuck in the neck between mother and bud, although tubulin staining revealed a typical mitotic spindle (Fig. 2*c*, middle inserts). By 24 hours, ~ 80% of cells were arrested in M phase; they had low Cdc28 activity and lacked Clb2 (data not

NIMA) 18,245 ase (kb) data not in Ess1/ alization al WW la). The s, occurs the WW ng a Pro- a protein domain. the newly similarity proteins entration- ulin[12], was gue (data s family of activity[15] motrypsin ast *CPR3*, ase has yet that Pin1/

is necessary ase domain alysis. Cells n for spore inal trunca- ions in three 57A, I159A) plement the gave similar ved that Pin1 as slightly less utant protein tro (Fig. 2b). se activity is

1 in yeast, we *PIN1* under ulated expres- ta not shown). normally in row in repres- iking terminal entation. Cell g to repressing f phase with 2n cells contained bud, although ndle (Fig. 2c; ; arrested in M Clb2 (data not

and Ess1 *S1* in yeast *ESS1* were trol vector, trads from segregation % of tetrads lemonstrat- ploid cells. e similar to xperiments, *ss1*⁻ diploid functionally that Pin1/

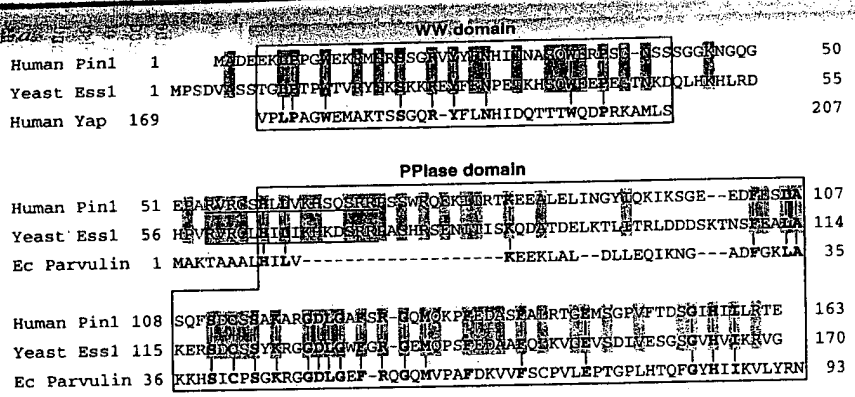

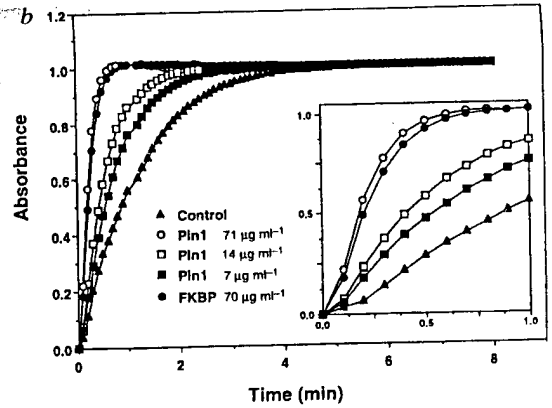

homology to Ess1, parvulin and Yap WW domain. *a*, Alignment of Pin1, Ess1, human Yap WW domain and *Escherichia coli* parvulin. Dashes indicate gaps, vertical lines indicate identity among all three sequences, and shaded boxes indicate identity between Pin1 and Ess1. Underlined residues form a consensus bipartite nuclear localization signal. *b*, Isomerase activity was monitored by a change in the absorbance at 395 nm, with the final stable absorbance of each sample being set at 1.0. Different concentrations of Pin1 were used as indicated, with FKBP PPIase as a control. The insert shows PPIase activity during the first minute of assay.

METHODS. For the yeast two-hybrid screen, *Aspergillus nimA* was fused to the GAL4 DNA-binding domain in the pAS2 vector[25]. Initially, Y190 cells were transformed with the NIMA/pAS2 expression vector but failed to produce stable strains, probably because overexpression of NIMA induces premature mitotic arrest in budding yeast, as it does in other eukaryotic cells[1,3,7,8]. Therefore NIMA was cotransformed with a HeLa cell cDNA library fused to the GAL4 activation domain[26], and screening was done as described[25]. Of 10^6 colonies screened, 13 showed a specific interaction with NIMA and belonged to three distinct gene classes, referred to as *PIN1*-3. Six clones contained cDNAs encoding *PIN1*, with different sequences between C − 9 and G + 15. Additional 5′ sequence was obtained by screening a HeLa cell cDNA library (from R. Fukunaga). To express the $(His)_6$-tagged Pin1 protein, *PIN1* cDNA was subcloned into pProEx1, and the recombinant protein was expressed in and purified from BL21 bacteria using Ni^{2+}-NTA agarose as described by the manufacturer (Qiagen). FKBP was provided by D. Schultz and C. Zuker. Isomerase activity was measured as described[27].

a

Plasmid	Total tetrads	Number of viable spores per tetrad 0	1	2	3	4	Cell doubling times (h)
Vector	21	0	3	17	1	0	No growth
PIN1	83	5	6	46	6	20	2.2*, 3.5^
ESS1	29	0	0	6	6	17	2.1*, 2.5^

b

Plasmid	Total tetrads	Number of viable spores per tetrad 0	1	2	3	4	PPIase activity
PIN1	44	2	1	25	6	10	+
PIN1-3A	48	0	2	46	0	0	-
PIN1-3′Δ	44	0	3	41	0	0	-

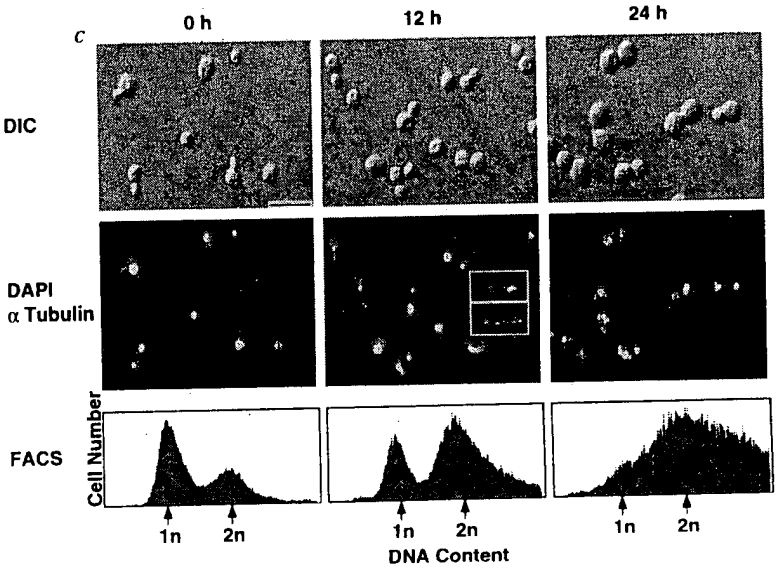

FIG. 2 *PIN1* functions as a mitotic regulator in yeast and its PPIase is required for cell viability. *a*, *PIN1* complements *ess1*⁻ yeast. Disruption strain MGG3/pSHU (*ess1::URA3*/*ESS1*)[14] was transformed with vector alone, or with plasmids expressing *PIN1* or *ESS1*. Cells were induced to sporulate, tetrads dissected, and the number of viable spores scored after 3 days. Doubling times were determined by growing *PIN1*- or *ESS1*-expressing *ess1::URA3* segregants in rich (*) or synthetic (^) media. *b*, Pin1's PPIase activity is required for function. MGG3/pSHU was transformed with plasmids expressing wild-type or PPIase mutant *PIN1*. Spore viability was analysed as in *a*. PPIase activity was assayed *in vitro* using a peptide substrate. *c*, Depletion of Pin1/Ess1 causes mitotic arrest and nuclear fragmentation. Pin1-dependent haploid cells (*ess1*⁻ *GAL–PIN1*) were shifted from inducing (galactose) to repressing (glucose) media, collected and fixed at the times indicated. Cells were stained with DAPI or anti-tubulin mAb (inset) and visualized by Nomarski (DIC) or fluorescent illumination. For FACS analysis, cells were stained with propidium iodide. Scale bar, 10 μm; insets show a higher magnification of DAPI (top) and α-tubulin (bottom) staining of a representative cell.

METHODS. For genetic complementation, *PIN1* cDNA was expressed from the constitutive yeast triose-phosphate isomerase promoter in 2μ vector, pJK305-TPI (provided by J. Kamens and R. Brent). PPIase mutants were expressed from the *GAL1* promoter in pBC103 (B. Cohen and R. Brent), and cotransformed with artificial activator GAL4-ER-VP16 (ref. 28) into MGG3/pSH-U, which is *gal2*⁻. Tetrads were dissected on plates containing 5×10^{-9} M β-oestradiol. Expression and PPIase assays were done as in Fig. 1*b*. Tubulin staining was done as described[29]. The Pin1-dependent *ess1*⁻ strain (YSH12) carries an integrated copy of the *PIN1* cDNA under control of the *GAL1* promoter.

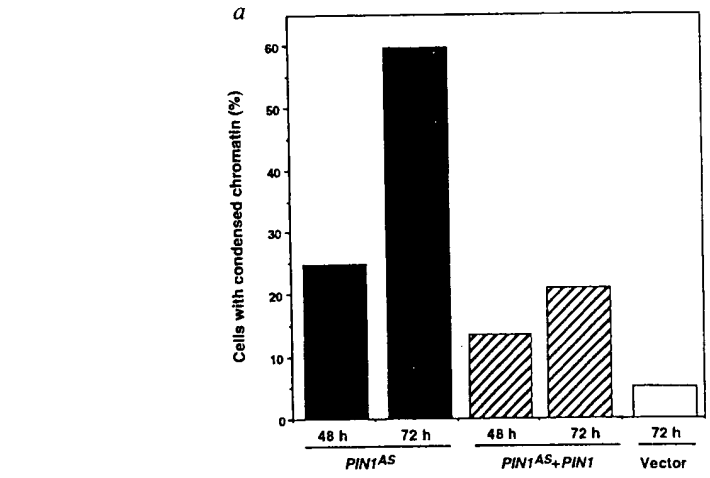

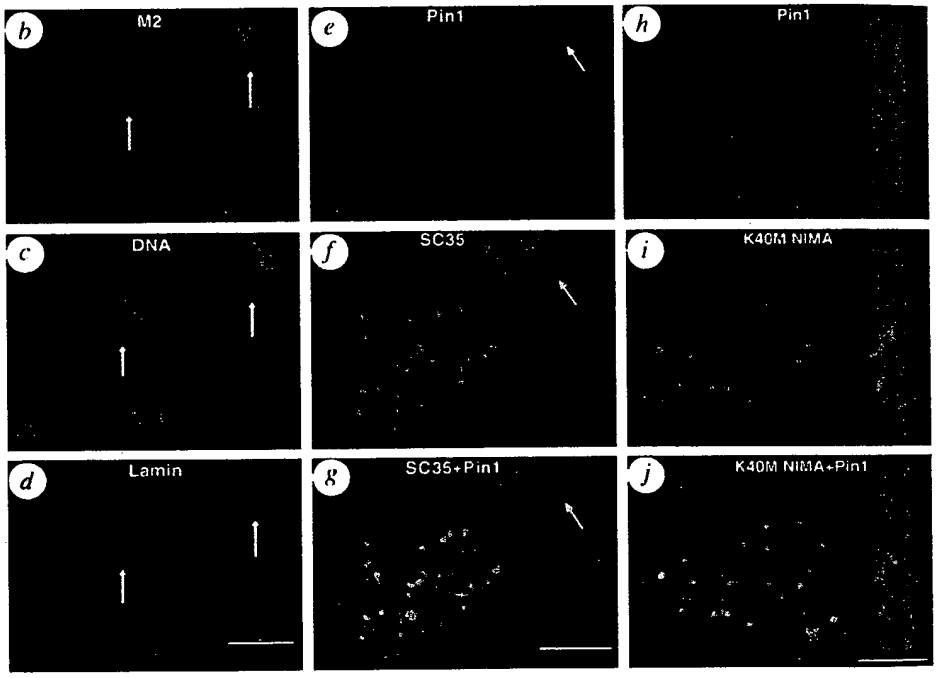

FIG. 3 Pin1 colocalizes with NIMA in the nuclear speckle and induces mitotic arrest when underexpressed in HeLa cells. *a*, tTA-1 cells were transfected with the indicated construct plus FLAG-tagged K40M NIMA280, which does not affect the cell cycle[7] and lacks the Pin1-interaction domain. Cells were stained with anti-FLAG tag M2 mAb and scored for cells with mitotic phenotype. In each case, at least 250 M2-positive cells were counted in random fields. *b–d*, tTA-1 cells transfected with $PIN1^{AS}$ plus FLAG-tagged K40M NIMA280 for 72 h were triply stained for transfected cells (*b*) using M2 mAb, for DNA (*c*) using Hoechst, and for the nuclear lamina (*d*) using anti-lamin A polyclonal antibodies. The arrows point to transfected cells identified by M2 staining for K40M NIMA280, which is localized in the Golgi complex. Scale bar, 5 μm. *e–j*, tTA-1 cells transfected for 24 h with the vectors expressing HA-tagged Pin1 alone (*e–g*), or plus FLAG-tagged kinase-negative K40M NIMA (*h–j*), were doubly stained for Pin1 using anti-HA tag 12CA5 mAb (IgG2b) and for SC35 using anti-SC35 mAb (IgG1) or NIMA using anti-FLAG tagged M2 mAb (IgG1). The two different antibody isotypes were probed with anti-IgG2b-Texas Red and anti-IgG1-FITC, respectively, followed by confocal microscopy. Double-staining for Pin1 and SC35 or NIMA was displayed by superimposing the respective images, with yellow indicating colocalization. Pin1 was also colocalized with wild-type NIMA in NIMA-induced mitotic cells (data not shown). Arrows point to an untransfected cell, indicating very little crossreactivity among the antibodies. Scale bar, 1 μm. METHODS. *PIN1* cDNA was subcloned into the pUHD-P2 vector so that it was expressed with a single N-terminal HA tag or into the pUHD-P1 vector in the antisense orientation ($PIN1^{AS}$), transfected into tTA-1 cells (a HeLa-derived cell line), followed by indirect fluorescence microscopy, as described[7].

shown), indicating that the arrest point was after cyclin B (Clb2) degradation. Arrested cells showed extensive nuclear fragmentation, accompanied by collapse of the mitotic spindle; this began at ~ 18 hours, and was essentially complete by 24 hours (Fig. 2*c*; data not shown). As expected, these phenotypes appeared earlier in cells that expressed lower initial Pin1 concentrations (data not shown). Thus depletion of Pin1/Ess1 induces mitotic arrest and eventual nuclear fragmentation, suggesting that Pin1/Ess1 is required to inhibit entry into M and/or to promote exit from M.

To examine Pin1 function in human cells, haemagglutinin (HA)-tagged *PIN1* and/or antisense full-length *PIN1* ($PIN1^{AS}$) was expressed in HeLa cells, followed by fluorescence microscopy and fluorescence-activated cell sorting (FACS) analysis, as described[7]. About 50% of cells overexpressing Pin1 arrested in G2, whereas control cells not expressing Pin1 (within the Pin1-transfected population) and vector-transfected cells displayed a normal cell-cycle profile (data not shown), indicating that overexpression of Pin1 inhibits the G2/M transition. In contrast, cells transfected with PIN^{AS} displayed mitotic phenotypes including cell rounding, chromatin condensation and nuclear-lamin disassembly (Fig. 3*b–d*). These phenotypes appeared 48 hours after transfection, and were evident in ~ 60% of cells by 72 hours, when the nucleus became fragmented in most cells. The $PIN1^{AS}$-induced mitotic phenotype was dramatically reduced by coexpression of sense *PIN1* cDNA. Because depletion of Pin1 in yeast also induced a similar phenotype, these results indicate that Pin1 and Ess1 have a highly conserved mitotic function.

The mitotic function of Pin1 prompted us to examine its subcellular localization. Pin1 was almost exclusively nuclear, with a speckled appearance (Fig. 3*e–g*). These speckles were identical to those detected using anti-SC35 splicing factor monoclonal antibody[19] (Fig. 3*e–g*). Thus Pin1 is associated with the nuclear speckle, which is a key component of the nuclear scaffold or matrix and undergoes disassembly in mitosis[20]; several other mitosis-related proteins are also associated with this structure. The fission yeast protein CDC28, required for M phase, is a splicing factor[21]. The yeast Dsk1 kinase, a suppressor of the mitotic *dis1* mutant[22], is homologous to a human mitotically active splicing factor kinase, Srpk1 (ref. 23), and overexpression of Dsk1 delays the G2/M transition[22]. These results suggest that the reorganization of the nuclear speckle may be needed for entry into M phase.

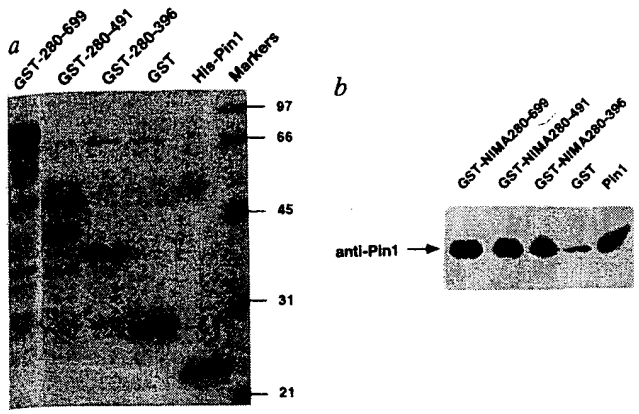

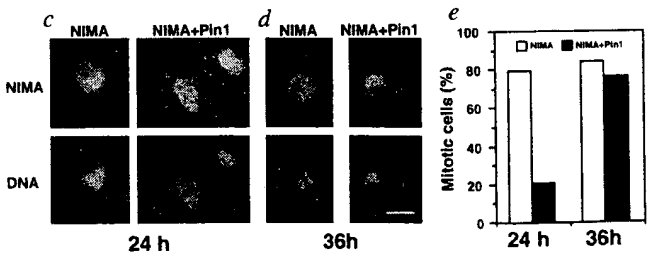

FIG. 4 Pin1 interacts with the NIMA essential protein-interacting domain (NID) and attenuates its mitosis-promoting activity when overexpressed in HeLa cells. *a*, *b*, Recombinant purified His–Pin1 and different glutathione *S*-transferase (GST)–NIMA fusion proteins were analysed by sodium dodecyl sulphate–polyacrylamide gel electrophoresis (SDS–PAGE) followed by Coomassie staining (*a*). GST–NIMA beads were incubated with His–Pin1 for 2 h and washed extensively. Pin1 bound to the beads was detected by Coomassie staining, followed by immunoblot analysis using Pin1-specific polyclonal antibodies (*b*). Based on Coomassie staining, about one-fifth of the Pin1 input was precipitated by each GST–NIMA protein. *c*–*e*, tTA-1 cells were cotransfected with FLAG–NIMA and HA–Pin1 or control vector for 24 (*c*) or 36 h (*d*) and stained with M2 mAb and Hoechst dye to examine the phenotype of NIMA-expressing cells under a fluorescence microscope. *e*, The percentage of cells with rounding and chromatin condensation scored in a sample of at least 250 M2-positive cells. Scale bar, 5 μm.

METHODS. *a*, *b*, The *PIN1* cDNA was subcloned into pET28a and different domains of NIMA[7] into a pGEX vector and the recombinant proteins were purified from bacteria using Ni^{2+}-NTA or glutathione-agarose column, as described[30]. *In vitro* binding was performed at 4 °C for 2 h in NP40 buffer (50 mM Tris-HCl, pH 8.0, 0.5% NP40, 200 mM NaCl, 20 mM β-glycerophosphate, 20 mM NaF, 0.1 mM sodium orthovanadate, 50 μg ml^{-1} phenylmethylsulphonyl fluoride, 10 μg ml^{-1} leupeptin, 10 μg ml^{-1} aprotinin) containing 1 mg ml^{-1} BSA, followed by washing 8 times with the buffer without BSA. Pin1 was detected by immunoblot analysis using Pin1 antibodies, which were generated in rabbits against the C-terminal 17 residues. The antibodies specifically recognised an 18K endogenous Pin1 protein in HeLa cell lysates. *c*–*e*, tTA-1 cells were cotransfected with FLAG–NIMA and HA–*PIN1* or vector for 24 or 36 h, followed by fluorescence microscopy, as described[7].

Manipulation of Pin1 or NIMA functions induces strikingly similar, albeit reciprocal, phenotypes, suggesting that they are in a common pathway. Dominant-negative mutant NIMA induces G2 arrest, whereas NIMA overexpression induces M arrest and nuclear fragmentation[1,3,5,8], with the arrest point being after cyclin B degradation if overexpressed in G2 (ref. 4). Pin1 specifically interacts with the NIMA C-terminal regulatory domain in the two-hybrid system (data not shown). *In vitro* assays using recombinant proteins indicated that, although Pin1 did not act as a substrate or a inhibitor of NIMA kinase (data not shown), it specifically interacted with residues 280–396 of NIMA (Fig. 4*a*, *b*), which has previously been shown to be essential for NIMA *in vivo* function and proposed to be a protein-interacting domain (NID)[5,7]. Furthermore, Pin1 and NIMA co-immunoprecipitated (data not shown) and colocalized in nuclear speckles in HeLa cells (Fig. 3*h*–*j*). Moreover, coexpression of Pin1 and NIMA attenuated NIMA mitosis-promoting activity (Fig. 4*c*–*e*). In addition, Pin1 was originally isolated by its ability to suppress the NIMA lethal phenotype in yeast (Fig. 1*a* legend). These results indicate that Pin1 binds the NID domain of NIMA and somehow inhibits its mitotic function. Because activation and inactivation of NIMA are required for entry into and exit from M, respectively[2,4,7], it is possible that Pin1 is involved in regulation of both these checkpoints, although we do not know whether Pin1 also has another role in exit from M.

Thus Pin1, a novel conserved PPIase, is an essential mitotic regulator, presumably in the NIMA pathway. Pin1/Ess1 is the first reported PPIase involved in cell-cycle control. The recent identification of a Pin1/Ess1 homologue in *Drosophila*, *dodo*, which functions in yeast[24], underscores the conserved nature of this protein. By using Pin1, it may be possible to identify functional homologues of NIMA in vertebrates. □

Received 23 January; accepted 20 February 1996.

1. Osmani, S. A., Pu, R. T. & Morris, N. R. *Cell* **53,** 237–244 (1988).
2. Osmani, A. H., McGuire, S. L. & Osmani, S. A. *Cell* **67,** 283–291 (1991).
3. Lu, K. P. & Means, A. R. *EMBO J.* **13,** 2103–2113 (1994).
4. Pu, R. T. & Osmani, S. A. *EMBO J.* **14,** 995–1003 (1995).
5. Lu, K. P. & Hunter, T. in *Progress in Cell Cycle Research* Vol. 1 (eds Meijer, L., Guidet, S. & Tung, H. Y. L.) 187–205 (Plenum, New York, 1996).
6. Fry, A. M. & Nigg, E. A. *Curr. Biol.* **5,** 1122–1125 (1995).
7. Lu, K. P. & Hunter, T. *Cell* **81,** 413–424 (1995).
8. O'Connell, M. J., Norbury, C. & Nurse, P. *EMBO J.* **13,** 4926–4937 (1994).
9. Schreiber, S. L. *Science* **251,** 283–287 (1991).
10. Heitman, J., Movva, N. R. & Hall, M. N. *New Biol.* **4,** 448–460 (1992).
11. Fischer, G. *Angew. Chem. int. Edn. engl.* **63,** 67–118 (1994).
12. Rahfeld, J. U. *et al. FEBS Lett.* **343,** 65–69 (1994).
13. Rudd, K. E. *et al. Trends biochem. Sci.* **20,** 12–14 (1995).
14. Hanes, S. D., Shank, P. R. & Bostian, K. A. *Yeast* **5,** 55–72 (1989).
15. Hani, J., Stumpf, G. & Domdey, H. *FEBS Lett.* **365,** 198–202 (1995).
16. Sudol, M. *et al. FEBS Lett.* **369,** 67–71 (1995).
17. Chen, H. I. & Sudol, M. *Proc. natn. Acad. Sci. U.S.A.* **92,** 7819–7823 (1995).
18. Davis, E. S. *et al. Proc. natn. Acad. Sci. U.S.A.* **89,** 11169–11173 (1992).
19. Fu, X. D. & Maniatis, T. *Nature* **343,** 437–441 (1990).
20. Spector, D. L. *A. Rev. Cell Biol.* **9,** 265–315 (1993).
21. Fu, X. D. *RNA* **1,** 663–680 (1995).
22. Takeuchi, M. & Yanagida, M. *Molec. Biol. Cell* **4,** 247–260 (1993).
23. Gui, J. F., Lane, W. S. & Fu, X. D. *Nature* **369,** 678–682 (1994).
24. Maleszka, R. *et al. Proc. natn. Acad. Sci. U.S.A.* **93,** 447–451 (1996).
25. Harper, J. W. *et al. Cell* **75,** 805–816 (1993).
26. Hannon, G. J., Demetrick, D. & Beach, D. *Genes Dev.* **7,** 2378–2391 (1993).
27. Heitman, J. *et al. Methods* **5,** 176–187 (1993).
28. Louvion, J. F., Havaux, C. B. & Picard, D. *Gene* **131,** 129–134 (1993).
29. Roberts, C. J. *et al. Meth. Enzym.* **194,** 644–661 (1991).
30. Lu, K. P., Osmani, S. A. & Means, A. R. *J. biol. Chem.* **268,** 8769–8776 (1993).

ACKNOWLEDGEMENTS. We thank X. D. Fu, J. Heitman, S. Forsburg, M. Latterich, J. Noel, H. Toyoshima and D. Nag for advice; G. Hannon, D. Beach, S. Elledge, X. D. Fu, R. Fukunaga, L. Gerace, M. D. Mendenhall and H. Bujard for reagents; D. Schultz and C. Zuker for help with the PPIase assay; R. Hackett for help with some yeast experiments; M. Latterich and G. Mondesert for help with tubulin staining; T. Murray, G. Karpen and R. Glaser for help with microscopy; V. Edelman and T. Deerinck for help with confocal microscopy; D. Chambers for help with FACS analysis; and Wadsworth Center Core Facilities for microscopy and oligonucleotide synthesis. The studies were supported by grants from Health Research Inc. (S.D.H.) and the USPHS (T.H. and M. Ellisman). K.P.L. is a Leukemia Society of America fellow, and T.H. is an American Cancer Society research professor.

CORRESPONDENCE and requests for materials should be addressed to K.P.L. (e-mail: Lu@SC2.Salk.Edu). The GenBank accession number for Pin1 is U49070.

ordered.
from JTIC
23 JUNE 2003.

1: FEBS Lett. 1995 Aug 1;369(1):67-71.

Characterization of a novel protein-binding module--the WW domain.

Sudol M, Chen HI, Bougeret C, Einbond A, Bork P.

Laboratory of Molecular Oncology, Rockefeller University, New York, NY 10021, USA.

We have identified, characterized and cloned human, mouse and chicken cDNA of a novel protein that binds to the Src homology domain 3 (SH3) of the Yes proto-oncogene product. We subsequently named it YAP for Yes-associated protein. Analysis of the YAP sequence revealed a protein module that was found in various structural, regulatory and signaling molecules. Because one of the prominent features of this sequence motif is the presence of two conserved tryptophans (W), we named it the WW domain. Using a functional screen of a cDNA expression library, we have identified two putative ligands of the WW domain of YAP which we named WBP-1 and WBP-2. Peptide sequence comparison between the two partial clones revealed a homologous proline-rich region. Binding assays and site-specific mutagenesis have shown that the proline-rich motif binds with relatively high affinity and specificity to the WW domain of YAP, with a preliminary consensus that is different from the SH3-binding PXXP motif. This suggests that the WW domain has a role in mediating protein-protein interactions via proline-rich regions, similar but distinct from Src homology 3 (SH3) domains. Based on this finding, we hypothesize that additional protein modules exist and that they could be isolated using proline-rich peptides as functional probes.

Publication Types:
- Review
- Review, Tutorial

PMID: 7641887 [PubMed - indexed for MEDLINE]

1: FEBS Lett. 1996 Apr 8;384(1):1-8.

ELSEVIER SCIENCE FULL-TEXT ARTICLE

Towards prediction of cognate complexes between the WW domain and proline-rich ligands.

Einbond A, Sudol M.

Department of Biochemistry, Mount Sinai School of Medicine, New York, NY 10029-6547, USA.

The WW domain is a structured protein module found in a wide range of regulatory, cytoskeletal, and signaling molecules. Its ligands contain proline-rich sequences, some of which show a core consensus of XPPXY that is critical for binding. In order to gain a better understanding of the molecular and biological functions of WW domains, we decided to predict their cognate ligands by searching databases for proteins containing the XPPXY consensus. Using several axioms that take into account evolutionary conservation and functional similarity, we have identified four groups of proteins representing candidate ligands that signal through known or unknown WW domains. These include viral Gag proteins, sodium channels, interleukin receptors, and a subgroup of serine/threonine kinases. In addition, we proposed that dystrophin and beta-dystroglycan bind through the WW-XPPXY link and that interference with this interaction could result in muscular dystrophy. Our study provides guidelines for experiments to probe the molecular and biological functions of the WW domain-ligand connection. Should these predictions be proven empirically, the results may have important ramifications for basic research and medicine.

Publication Types:
- Review
- Review, Tutorial

PMID: 8797792 [PubMed - indexed for MEDLINE]

Structure and function of the WW domain.

Sudol M.

Mount Sinai School of Medicine, New York, NY 10029, USA.

Publication Types:

- Review
- Review, Academic

PMID: 9029943 [PubMed - indexed for MEDLINE]